NANO LETTERS

Letter

pubs.acs.org/NanoLett

Nanoengineered Surfaces for Focal Adhesion Guidance Trigger Mesenchymal Stem Cell Self-Organization and Tenogenesis

Maria Iannone,[†,‡] Maurizio Ventre,[†,‡] Lucia Formisano,[†,‡] Laura Casalino,[§] Eduardo J. Patriarca,[§] and Paolo A. Netti*[,†,‡]

[†]Center for Advanced Biomaterials for Healthcare@CRIB, Istituto Italiano di Tecnologia, Largo Barsanti e Matteucci 53, 80125 Naples, Italy

[‡]Department of Chemical, Materials and Industrial Production Engineering and Interdisciplinary Research Centre on Biomaterials, University of Naples Federico II, P.le Tecchio 80, 80125 Naples, Italy

[§]Stem Cell Fate Laboratory, Institute of Genetics and Biophysics "A. Buzzati-Traverso", National Research Council, Via Castellino 111, 80131 Naples, Italy

Supporting Information

ABSTRACT: The initial conditions for morphogenesis trigger a cascade of events that ultimately dictate structure and functions of tissues and organs. Here we report that surface nanopatterning can control the initial assembly of focal adhesions, hence guiding human mesenchymal stem cells (hMSCs) through the process of self-organization and differentiation. This process self-sustains, leading to the development of macroscopic tissues with molecular profiles and microarchitecture reminiscent of embryonic tendons. Therefore, material surfaces can be in principle engineered to set off the hMSC program toward tissuegenesis in a deterministic manner by providing adequate sets of initial environmental conditions.

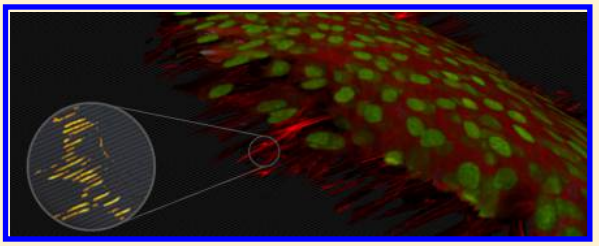

KEYWORDS: *Stem cell, nanopattern, focal adhesions, tenogenic differentiation, self-organization, tissue development*

Morphogenetic events are launched by initial conditions defined by the physicochemical characteristics of the environment. The sequence of processes that occurs afterward propagates with an astonishing consistency and terminates with the establishment of highly complex tissue structures. During the last decades, much effort was dedicated to unravel the mechanisms behind morphogenesis with the belief that these would have suggested inspiring strategies to tackle unsolved problems such as the treatment of degenerative pathologies and the replacement of injured tissues. Major breakthroughs in this field have recently regarded the in vitro development of organoids such as brain, intestine, and optic-cup,[1−3] which paved the way for the use of organoids systems as developmental and disease models or for drug screening.[4,5] These studies rely on the spontaneous spatial self-organization and differentiation of embryonic stem cells (ESCs) or induced pluripotent stem cells (iPSs) spheroids, which if cultivated in specific conditions, mostly in low attachment or suspension, evolve in complex assemblies displaying remarkable structural and molecular similarities with native tissues and organs. However, very little is known on the influence of the initial physical interactions with the surrounding environment on the morphogenetic process. For instance, the physical properties of the supporting extracellular matrix (ECM) in the form of microstructure and stiffness are known to control and guide specific morphogenetic events.[6] It is therefore possible that exogenous physical stimuli might control and guide the self-organization process, thus providing an adequate microenvironment, which eventually dictates form and functions of supracellular structures. In particular, focal adhesions (FAs) are the mechanical links with the extracellular environment and are mainly responsible for the outside-in and inside-out transmission of forces.[7] These forces not only are crucial for the establishment of the tissue morphology but also regulate cell differentiation through specific mechanostransduction pathways.[8] Indeed, several studies exploiting material surfaces able to modulate cell contractility through FA formation and growth demonstrated that physical signals potently control cell fate and functions.[9−11] However, these studies provided little insight into the role of FA formation and cell generated forces on tissue formation. Here we demonstrate that by exploiting material surface nanopatterning it is possible to control the initial spatial positioning and growth of FAs that ultimately dictate tissue formation: from cell self-organization down to differentiation in a deterministic manner. In particular, human mesenchymal stem cells (hMSCs), cultivated on polydimethylsiloxane (PDMS) substrates with arrays of parallel channels having 700 nm width and 1.4 μm pitch (Figure 1a and Supporting Information Figure S1a) without exogenously added growth factors, are guided through the process of self-

Received: September 29, 2014
Revised: February 16, 2015

DOI: 10.1021/nl503737k
Nano Lett. XXXX, XXX, XXX−XXX

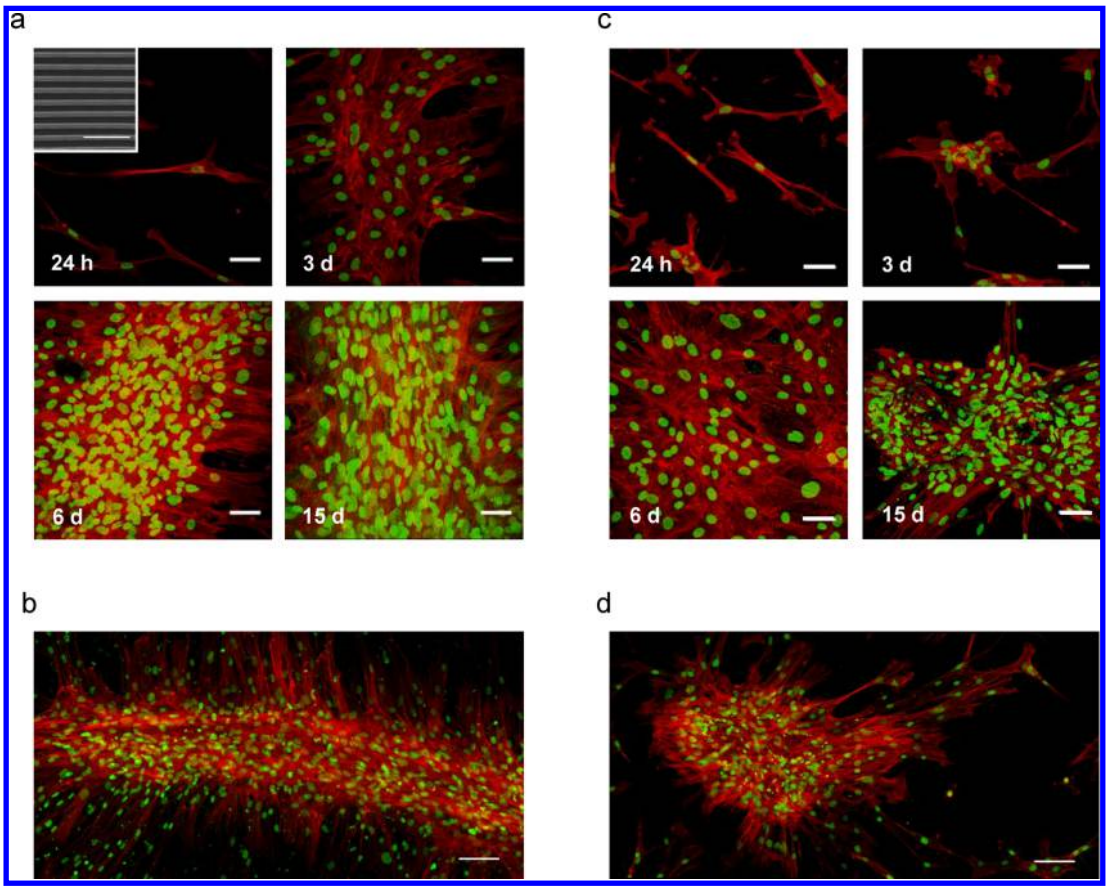

Figure 1. Genesis and formation of tendon-like supracellular structures. (a) Confocal images of hMSCs cultivated on the 1.4 μm pitch patterned PDMS (inset) at different time points. At 24 h, hMSCs elongated along the pattern direction (horizontal axis). After 3 days of culture, cell aggregates spontaneously formed zipper-like structures directed across the pattern direction. The zipper-like structures steadily increased their width and length (6 days). After 15 days, hMSCs formed 3D constructs in which stem cells were densely packed and strongly aligned. (b) Confocal tile scan of tendon-like structure after 15 days of culture on the 1.4 μm pitch patterned substrate. (c) Confocal images of hMSCs cultivated on flat substrates. Cells initially adhered and elongated (24 h) but assembled in randomly oriented clusters (3 and 6 days), which eventually formed spherical aggregates with no macroscopic order (15 days). (d) Confocal tile scan of a spherical cell aggregate after 15 days of culture on flat substrate. Nuclei are displayed in green and the cytoskeleton in red. Scale bar is 50 μm in panels a and c and 100 μm in panels b and d.

organization and differentiation, which led to the development of 3D tissues with cellular and extracellular matrix organization closely resembling that of an embryonic human tendon. Tissue formation follows a precise and reproducible time sequence. First, cells seeded at low density on the patterned surface exhibited a strong polarization along the pattern direction and migrated preferentially along it (Figure 1a, Supporting Information Figure S2a and see Video 1 in Supporting Information). On day 3 postseeding, hMSCs formed cell aggregates oblong in shape and with the long axis predominantly directed perpendicularly to the pattern (Figure 1a and Supporting Information Figure S2a). From day 3 to day 6, the scattered aggregates gathered and merged forming elongated structures (Figure 1a, Supporting Information Figure S2a and see Video 2 in Supporting Information). A considerable recruitment of cells within the structures was observed from day 6 (see Video 3 in Supporting Information). This caused the structures to become thicker and densely populated and a concurrent structure straightening was observed in this time frame. On day 7, several long and straight structures were visible on the nanopatterned surface. Furthermore, cells within the structures were clearly located on different planes, thus forming a 3D cylindroid. Such a cellular assembly suggested the existence of a provisional scaffolding matrix. Indeed, hMSCs are known to synthesize collagen in vitro,[12] and to retain the collagen produced culture medium was supplemented with ascorbic acid. Interestingly, ascorbic acid supplemented at day 0 did not allow the formation of the long and straight supracellular structures (data not shown). From day 7 onward, the structures kept growing owing to cell recruitment from the surroundings or the merging of two sufficiently close structures (Supporting Information Figure S3a and see Video 4 in Supporting Information). On day 15, the nanopattern was mostly populated by macroscopic, cylindrical structures (Figure 1a,b and Supporting Information Figure S2a). Conversely, the hMSCs seeded on a flat surface displayed neither a macroscopic alignment, nor a directed migration. From day 1 to day 3, the flat surface induced the formation of spherical cell aggregates that occasionally fused together (Figure 1c and Supporting Information Figure S2b and see Video 5 in Supporting Information). However, such cell aggregates never developed into ordered supracellular structures (Figure 1d and Supporting Information Figure S3b).

This peculiar dynamics suggested the hypothesis that the modulation of FA growth and spatial positioning mediated by the nanopattern controls the cytoskeletal assembly of the cell at the initial adhesion stage that in turn sequentially affects collective cell behavior guiding the tissuegenesis process. Once

DOI: 10.1021/nl503737k
Nano Lett. XXXX, XXX, XXX−XXX

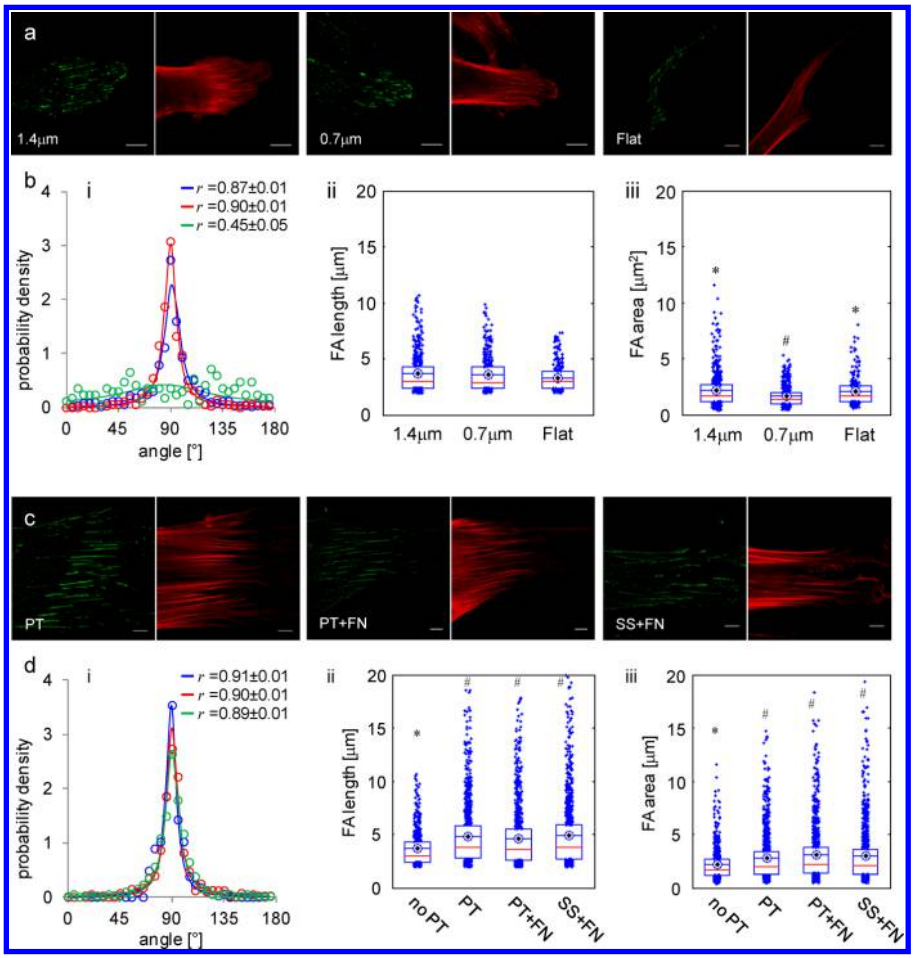

Figure 2. Surface modulation of hMSC adhesion and its effect on self-organization. (a) Confocal images of FAs and cytoskeleton assemblies of hMSCs cultivated for 24 h on 1.4 μm pitch patterns, 0.7 μm pitch patterns, and flat surfaces. FAs were stained for vinculin (green) and actin bundles were stained with TRITC-phalloidin (red), scale bar 10 μm. (b, i) Distribution of FA orientation. Open circles are the experimental data, solid lines are the wrapped Cauchy distribution fits over the experimental data (blue 1.4 μm pitch pattern n = 507; red 0.7 μm pitch pattern n = 366; green flat substrate n = 278). Pattern direction is at 90°. The values of the MLE scale factor r are reported in the top right corner as mean ±95% CI. (b, ii) Box plot of the focal adhesion length. (b, iii) Box plot of the focal adhesion area. Box edges define the 1st and 3rd quartile. Red line represents the median, whereas the blue target is the mean value. Columns not marked with the same symbol are significantly different ($p < 0.05$). (c) Confocal images of the FAs and cytoskeleton as in (a) for the 1.4 μm pitch patterned substrate treated with oxygen plasma (PT), 1.4 μm pitch patterned substrate treated with oxygen plasma and coated with fibronectin (PT+FN), and 1.4 μm pitch patterned substrate with covalently conjugated fibronectin through Sulfo-SANPAH cross-linker (SS+FN). (d, i) Distribution of FA orientation (blue PT n = 955, red PT+FN n = 883, green SS +FN n = 1065). (d, ii) Box plot of the focal adhesion length. (d, iii) Box plot of the focal adhesion area. Columns not marked with the same symbol are significantly different ($p < 0.05$).

started, maturation and growth of these structures required extensive cell remodelling in the form of cell dragging and zipper fusion, which is mediated by cell adhesion on the substrate. In order to verify this hypothesis, we investigated the combined effect of adhesivity and contractility on structure formation and growth. In more details, we altered these through either the chemical/geometrical modification of the nanopatterned surfaces or by the addition of specific inhibitors. First, we depressed FA growth and maturation by using nanopatterns displaying narrower features (with respect to the 1.4 μm pitch pattern), namely 350 nm wide ridges and 0.7 μm pitch (Supporting Information Figure S1b). On the 1.4 μm pitch and 0.7 μm pitch patterned substrates, as well as on the flat surfaces, hMSCs displayed vinculin-rich FAs and a well-defined cytoskeleton (Figure 2a). On the 0.7 μm pitch patterned substrates, FAs retained the same alignment (Figure 2b i) and length (Figure 2b ii) observed on the 1.4 μm pitch patterned substrates, although their area was significantly smaller (Figure 2b iii), thus indicating that the 0.7 μm pitch patterned substrates decreased local attachment. Notably, under these conditions the hMSCs occasionally generated circular aggregates but not ordered supracellular structures (Supporting Information Figure S4a).

Second, we promoted FA growth by treating the 1.4 μm pitch patterned substrates with oxygen plasma (PT), fibronectin coating after oxygen plasma (PT+FN) and fibronectin covalent conjugation through Sulfo-SANPAH linker (SS+FN) (Figure 2c). On the treated substrates, the FAs were highly coaligned with the pattern direction (Figure 2d i) and were significantly longer and larger with respect to the untreated case (Figure 2d, ii and iii). These treatments improved local attachment preserving FA orientation. However, when cultivated on treated surfaces the hMSCs generated a dense monolayer and were unable to form zipper-like supracellular structures (Supporting Information Figure S4b). After day 10, the hMSCs spontaneously formed zones with a

DOI: 10.1021/nl503737k
Nano Lett. XXXX, XXX, XXX−XXX

higher cell density nearly orthogonal to the pattern direction (Supporting Information Figure S4b); these, however, never developed into mature and thick structures as those observed in the untreated case. Therefore, nanopattern-induced FA confinement and polarized cell contractility appeared to be necessary for the induction of ordered supracellular structures, as their formation was not observed on flat surfaces. Moreover, an adequate level of cell attachment was required to enable cell self-organization, as hMSCs forming long and extended FAs did not produce ordered supracellular structures.

In order to modulate cell contractility, we inhibited Rho-associated protein kinase (ROCK) or myosin light chain by supplementing the culture medium with either Y-27632[13] or ML-7[14] from day 0 onward. In presence of either inhibitor, hMSCs on the 1.4 μm pitch pattern displayed an immature cytoskeleton with the vinculin markedly diffused in the cytoplasm (Supporting Information Figure S5a). Furthermore, the formation of zippers was not observed after 6 days of treatment (Supporting Information Figure S5b and see Videos 6 and 7 in Supporting Information). Only at longer times (10–15 days), the cells organized aggregates similar to those generated on the untreated nanopatterns, even though they appeared thinner and lacked the characteristic cellular orientation (Supporting Information Figure S5b,c). To assess whether contractility affected cell proliferation, in which case the delayed formation of structures could have arisen from a reduced cell number, we counted the cells cultivated on the 1.4 μm pitch pattern either in presence or in absence of the inhibitors up to 15 days. We found that inhibitors did not have any influence on cell proliferation up to 7 days (Supporting Information Figure S6a), a time frame in which we did not observe the formation of either the zipper or the supracellular structures, thus suggesting that the major role for structure formation is played by a coordinated contractility rather than cell density. Interestingly, when the inhibitors were added from day 7 onward, the already formed supracellular structures maintained their usual orientation perpendicular to the pattern direction (Supporting Information Figure S6b).

The self-organized structures developed on 1.4 μm pitch patterned substrates shared similarities with the tendon tissue, both in terms of macroscopic morphology and internal cellular organization. In order to gain a better insight into the spatial organization of the microconstituents, we used Picrosirius Red to analyze the samples at selected time points under polarized light. Collagen production was observed already after 24 h of ascorbic acid addition (7 days post seeding), both inside and around the structures (Figure 3a). An increase in collagen production was evident after additional 48 h of culture with ascorbic acid (9 days post seeding, Figure 3b). Later on, the staining intensity strongly increased within the structure, whereas the collagenous matrix on the nanopattern vanished. After 9 days of culture with ascorbic acid (15 days post seeding) the pattern was predominantly populated by long and intensely stained cylindrical structures (Figure 3c and Supporting Information Figure S7a). Notably, actomyosin inhibition reduced the signal detected under polarized light significantly. This occurred both when the inhibition was performed at the beginning of the cell culture or at 7 days, which we considered as the onset of tissue maturation (Supporting Information Figure S7b–e). Even though hMSCs self-organized in structures that morphologically resembled those that formed in normal culturing conditions, matrix production and assembly was dramatically altered, and this is consistent with the role of

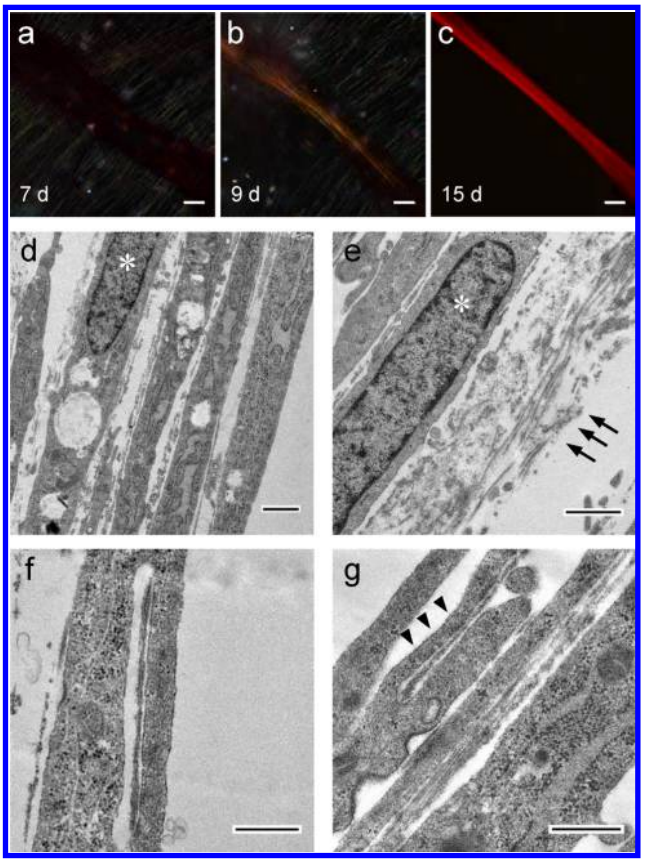

Figure 3. Collagen organization within the supracellular structures. (a) Picrosirus Red staining of hMSCs, seeded onto 1.4 μm pitch patterned surfaces, visualized in polarized light. After 24 h culture with ascorbic acid (7 days in total) hMSCs produced a thin and immature collagen layer, whose fibers (in green) were parallel to the pattern direction (~45° with respect to the horizontal axis). (b) After additional 48 h of culture with ascorbic acid (9 days in total), the collagen synthesized by cells appeared in bright orange indicating the presence of more mature fibers, which were assembled in bundles oriented perpendicular to the pattern forming the tendon-like structures. (c) After 9 days of culture with ascorbic acid (15 days in total), the fibers, compacted and aligned, appeared in an intense red stain, denoting a greater level of collagen maturation when observed under polarized light. Scale bar 100 μm. (d–g), Transmission electron micrographs of the tendon-like structures. (d) Cells' bodies and nuclei (white asterisk) in the inner part of the central shaft of the structure display a high degree of coalignment, which coincides with the long axis of the structure. (e) Intercellular zones are rich in fibrillar matrix whose orientation followed cell contours (black arrows). (f) Occasionally fibrillar matrix appeared within intracellular compartments, whereas extracellular matrix was frequently observed in deep recesses of the plasma membrane (black arrowheads). Scale bar 1 μm (d,e) and 500 nm (f,g).

the actomyosin machinery in the assembly and remodeling of collagen fibrils.[15,16]

TEM examinations were performed to investigate possible interplays between hMSCs and the de novo synthesized matrix after 15 days of culture. Longitudinal sections of the central part of the shaft of the structures that formed on the 1.4 μm pitch pattern, showed cells closely packed in the form of parallel arrays (Figure 3d). Nuclei also displayed an elongated morphology (Figure 3d,e). In many cases, we observed bundles of tiny filaments, presumably actin fibers, running in parallel to the nuclear and cytoplasmic membrane (Supporting Information Figure S8a). In the intercellular regions, a densely packed

DOI: 10.1021/nl503737k
Nano Lett. XXXX, XXX, XXX–XXX

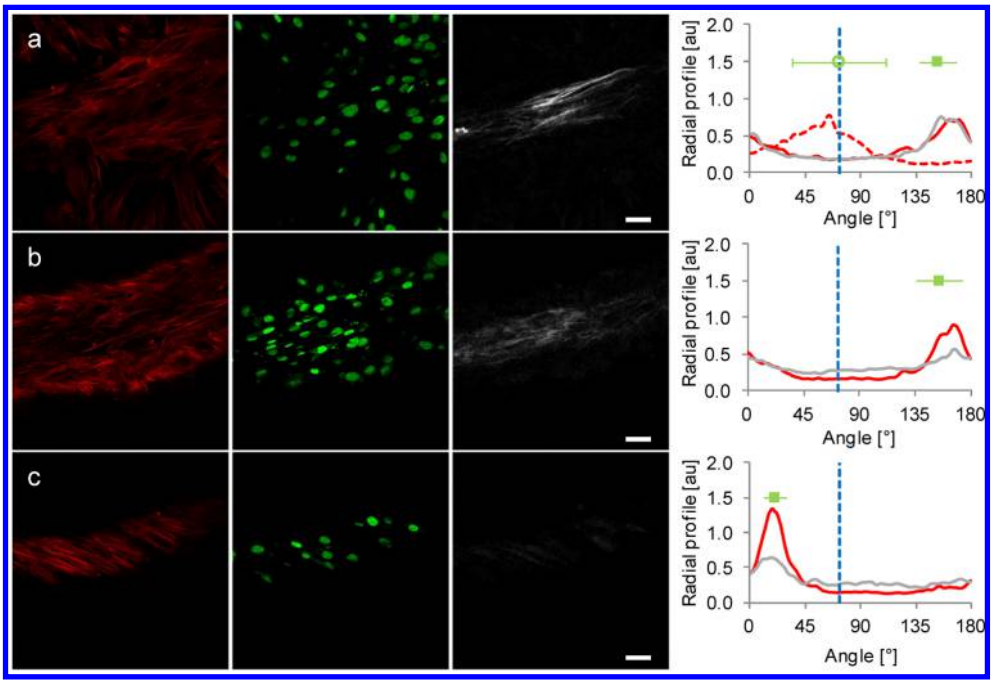

Figure 4. Spatial configuration of cells, nuclei, and collagen in 3D structures formed on the 1.4 μm pitch pattern. Actin (red), nuclei (green), and collagen (gray) were visualized at different focal planes within the tendon-like structures. (a) Cells in close contact with the pattern displayed a bimodal distribution of the orientation of cytoskeleton and nuclei. Cells outside the structure preserved the coalignment with the pattern, whereas cells and the collagen within the zipper were closely packed in the direction orthogonal to the pattern. The analysis of the orientation in terms of the FFT power spectrum radial profile of the TRITC-phalloidin and SHG signals is reported on the right. The red dashed and solid lines represent the orientation of the cells outside and inside the structure, respectively. The gray line is the orientation of collagen fibrils visible only inside the zippers. Nuclei orientations were quantified as the orientation of the major axis of the best fitting ellipse. The open circle and solid square indicate the orientation of the nuclei outside and inside the zipper, respectively. The blue dotted line is the pattern direction. (b,c) Orientation of the actin network, nuclei and collagen fibrils, in focal planes at 10 and 20 μm above the patterned substrate, respectively. Quantification of the orientation is reported in the right column and symbol designation is as in a. Scale bar = 20 μm.

fibrillar matrix followed cell contours (Figure 3e). Most fibrils were straight and directed along the 3D structure long axis. Occasionally, we also observed shorter fibrils originating in deep plasma membrane recesses or enclosed within cell compartments (Figure 3f,g), possibly suggesting an active role of cells in remodelling the ECM at this stage of tissue maturation.[16] However, cells constituting the outer shell had a less regular morphology, displaying several cytoplasmic vacuoles containing electron dense spots, similar to glycogen rosettes (Supporting Information Figure S8b). Interestingly, we frequently observed lamellar bodies, alone or in close proximity to vacuoles (Supporting Information Figure S8c,d). These structures are usually observed in those anatomical compartments that require some sort of lubrication.[17] In the case of articular joints, lamellar bodies are found in specialized fibroblast-like cells, namely type B synoviocytes, in the synovial intima that is closely connected to the tendon sheath.[18] These cells produce the synovial fluid that allows tendon gliding into the sheath cavity. Even though we do not have a thorough ultrastructural and molecular characterization of each and every cell type that constitute the in vitro produced tendon-like structure, it is tempting to speculate that a fraction of cells, in particular those located in the outer shell of the tendon-like structure, differentiate in order to synthesize the correct microenvironment to allow the tissue to became mechanically competent. Ultrastuctural images of hMSC aggregates formed on flat substrates displayed different morphological features both intracellularly and in the extracellular compartments. First, hMSCs were neither densely packed nor elongated (Supporting Information Figure S8e). A large number of spherical vacuoles populated the cytoplasm; most of them were predominantly located by the cell membrane (Supporting Information Figure S8f). No lamellar bodies were observed among these structures. Nuclei were not elongated and displayed a convoluted membrane (Supporting Information Figure S8g). Matrix was present in the extracellular space in the form of a disorganized network (Supporting Information Figure S8h).

These data were confirmed by second harmonic generation (SHG) microscopy that showed aligned collagen fibrils that became clearly visible from day 10 onward (Supporting Information Figure S9a). This enabled us to obtain information on the relative positioning of cells and collagen fibrils/fibers within and around the supracellular zipper-like structures that formed on the 1.4 μm pitch pattern. Z-stacked confocal images of 12 day old samples stained with TRITC-phalloidin and Sytox green revealed site-specific cellular assemblies within the structure. In particular, image analysis of the cells located on the bottom of the cylindrical structures, and thus in contact with the nanopatterned substrate, showed that their nuclei and cytoskeleton were aligned perpendicularly to the pattern direction. Collagen fibrils, observed in SHG mode, formed a dense matrix around the cells with almost the same orientation as the cell cytoskeleton (Figure 4a). As higher focal planes were visualized, cells and nuclei strongly coaligned with the collagen matrix and the direction of orientation was nearly perpendicular to the underlying pattern (Figure 4b). Interestingly, cells forming the outer shell were tilted of approximately 35° with

DOI: 10.1021/nl503737k
Nano Lett. XXXX, XXX, XXX−XXX

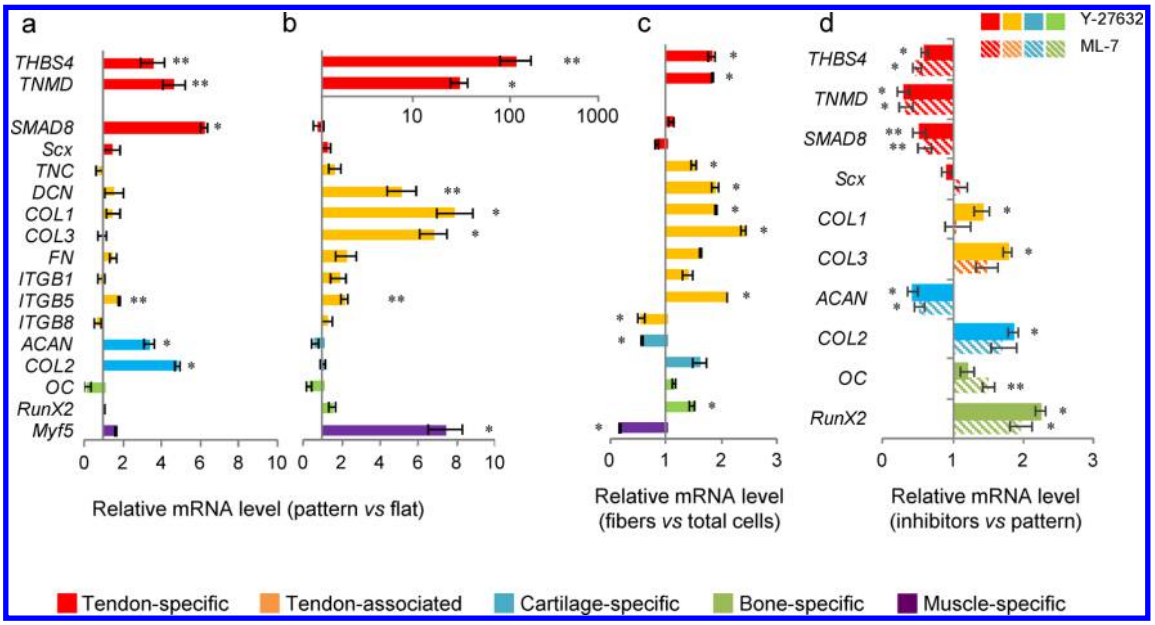

Figure 5. Effect of substrate matrix on tenogenic differentiation of human MSCs cultivated on 1.4 μm pitch pattern. RT-PCR analysis of the expression at 10 days (a) and 15 days (b) of representative genes specific for tenogenic differentiation (THBS4, thrombospondin 4; TNMD, tenomodulin; SMAD8, Scx, scleraxis), tendon matrix genes (TNC, tenascin C; DCN, decorin; COL1, collagen 1; COL3, collagen 3), tendon-associated adhesion molecules (FN, fibronectin; ITGB1, integrin β1; ITGB5, integrin β5; ITGB8 integrin β8) and chondrogenic (COL2, collagen 2; ACAN, aggrecan), osteogenic (RunX2; OC, osteocalcin F) and myogenic (Myf5, Myogenic Factor 5) differentiation markers. Relative gene expression was quantified using the $2^{-\Delta\Delta CT}$ method by normalizing the target gene expression to GAPDH and reported in histograms as relative fold change with respect to the flat substrate. Data are shown as mean ± SEM. Significant differences were assessed through two-tailed unpaired t-test (* $p < 0.001$; ** $p < 0.01$). For the complete list of oligonucleotide primers see Supporting Information. (c) Expression of markers within isolated fiber structures compared to the whole plate cells (fiber and extra-fiber cells) at 15 days of hMSCs on pattern substrate. (d) Effect of 15-day treatment with either ML-7 or Y-27632 on the hMSC differentiation onto 1.4 μm pitch pattern.

respect to the main axis of the zipper-like structures (Figure 4c).

Supracellular self-organization has been reported for different cell types. In particular, vascular mesenchymal cells form random labyrinthine structures in vitro around which cells are consistently directed perpendicular to the axis of the supracellular aggregate.[19] Also for this cell type, contractility was demonstrated to play a central role in structure formation and in determining the mutual orientation of cells within and outside the structures.[20] This suggests a possible common mechanism for diverse cell types to generate macroscopic patterns in vitro.

We therefore investigated the behavior of other cell types (NIH3T3, MG63, HDF, MC3T3) on the nanopatterned PDMS. Generally, cells adhered to the 1.4 μm pitch patterned substrate and coaligned with the pattern direction. However, cells reached a confluent state in 6 days of culture but no macroscopic supracellular structures were observed within this time frame (Supporting Information Figure S10).

Altogether, these data suggested that surface nanopatterning can induce hMSC differentiation toward a tenogenic path. To confirm this hypothesis, we analyzed the expression of tenogenic early and late markers by RT-PCR along with tendon-associated adhesion and matrix molecules. The results indicated that at 10 days the expression of the early tendon-specific (SMAD8) was 6-fold significantly higher in cells grown on the 1.4 μm pitch pattern compared to flat surface (Figure 5a), while the late tendon-specific markers (tenomodulin and thrombospondin 4) reached the maximal up-regulation later, at 15 days (31- and 110-fold, respectively) in which case we also observed an increased expression of the tendon-related genes decorin (5-fold), collagen-I (8-fold), and collagen-III (7-fold) (Figure 5b). Other non tendon-associated genes were significantly up-regulated at 10 days (aggrecan 5-fold and collagen II 3.5-fold) and at 15 days (myogenic factor 5, 7-fold). This is consistent with the hMSCs differentiation potential toward mesodermal-derived fates. More interestingly, when analyzing the expression of genes involved in tendon development only in the cells making up the structures, we found that the expression of tendon-specific and -associated genes was about 2-fold higher in isolated fibers compared with the total cell population adhering to the pattern surface; we also noticed a decrease of nontendon-related genes aggrecan and myogenic factor 5 (Figure 5c). Even though a few nontendon-related markers were still expressed in the structures, their overall expression levels with the exception of myogenic factor 5 were still very low (Figure 5b). The evidence of the overexpression of the tendon-specific and -associated genes suggests therefore that the tendon-like structures generated a microenvironment supportive of the predominant tenogenic differentiation with the up-regulation of late tendon markers. Cells on the nanopattern that do not constitute the tendon-like structures are likely to differentiate toward other mesodermal lineages.

Taken together, the molecular analysis supports the hypothesis of tenogenic differentiation mediated by the nanopattern, which defines the initial condition for adhesivity and therefore controls contractility. As expected, the inhibition of actomyosin contractility with ML-7 and Y-27632 induces a dramatic down-regulation of specific tendon markers (Figure 5d).

DOI: 10.1021/nl503737k
Nano Lett. XXXX, XXX, XXX−XXX

Our data confirm that the initial adhesive conditions provided by the nanopattern modulate the direction and magnitude of cell generated forces, eventually guiding cell self-organization and the development of highly ordered supracellular structures. Remarkably, the 1.4 μm pitch, but not the 0.7 μm pitch-patterned substrate, along with the adhesivity of the hydrophobic PDMS guarantees such a stringent balance. In particular, the nanopattern should initially confine and orient FAs in order to polarize the direction of cell contractile forces. However, the FA area should be sufficiently large to enable the adhesion of the cells, while allowing collective cell migration during the phases of zipper formation and structure organization.

In this work, we demonstrated that surface nanopatterning is effective in directing cell self-organization, which culminates in the in vitro generation of centimeter-long and viable tendon-like tissues without the employment of growth factors or exogenous scaffold matrices. While the effect of nanopatternig has been widely investigated in the context of cell differentiation, it has been rarely exploited to regulate cell self-organization thus obtaining tissues with predetermined architecture and functions. For example, Guillemette et al.[21] cultivated corneal fibroblasts on microtextured substrates and produced corneal equivalents displaying a lamellar micro-architecture similar to that found in native tissues and superior optical properties compared to corneal tissue grown on flat substrates. Kim et al.[22] successfully reproduced in vitro functional myocardial tissues by cultivating rat ventricular myocytes on nanotextured polyethylene glycol based materials. Strikingly, cells responded with great sensitivity to the nanometric features of the pattern by adapting their morphological, molecular, and electrophysiological characteristics. This emphasized the powerful role that nanoscale signals may have in modulating various aspects of the tissue behavior. More recently, Xing et al.[23] used synthetic nanogratings to produce aligned nanofibrous tissues that showed excellent properties in supporting hMSC growth and in mitigating inflammation response when used as a supporting scaffold. Therefore, nanopatterning can in principle dictate the micro-architecture of growing tissues and eventually their functions. However, information on the dynamics of cell self-organization and how this is regulated by the nanopatterned signals is still missing. We reported that the guiding power of surface nanopatterning goes well beyond tissue architecture. In fact, the nanopattern coordinates cell self-organization and defines the shape of the supracellular structures, whereas an intermediate level of adhesivity enables tissue remodelling. In fact, when failing to provide them with the adequate initial cues, hMSCs do not form ordered tendon-like tissues. For instance, increasing cell−substrate adhesivity with chemical treatments favors the formation of cell monolayers. Conversely, depressing adhesivity with narrower pattern features (0.7 μm pitch) promotes cell clustering in the form of spheroids. Other strategies, having the common purpose of modulating adhesivity, provided analogous results. For instance, stiffer 1.4 μm pitch patterned PDMS or hard 1.4 μm pitch patterned polycarbonate substrates lead to monolayer formation, whereas softer 1.4 μm pitch patterned PDMS substrates produced spherical clusters (Supporting Information Figure S4c, d). Likewise, the inhibition of cell contractility alters the morphology of supracellular structures and tissuegenesis and, additionally, reduces the expression of tendon-specific genes (Figure 5d). Interestingly, if inhibition starts at a point halfway the tenogenesis process, the gross structural morphology is retained (Supporting Information Figure S6b); however, the inner matrix is less ordered with respect to the untreated case (Supporting Information Figure S9b,c) and the expression of tendon specific and associated markers is altered (data not shown).

In the context of in vitro tenogenesis, diverse approaches have been pursued. Usually, these share the common principle that external anchors, which exert their action on a millimeter/centimeter length scale, constrain cell contractility and tissue compaction along a specific direction. In particular, Calve et al.[24] and Hairfield-Stein et al.[25] used tendon-derived primary fibroblasts and bone marrow stromal cells, respectively, on laminin-coated PDMS with macroscopic internal anchors, which exerted traction forces on cell aggregates by balancing cell contractility. Tissues displayed a collagen rich fibrous matrix and mechanical behavior in qualitative agreement with native tendons. Interestingly, nonplasma-treated PDMS in principle provides the cells with a level of attachment analogous to the one we exploited, which is necessary to enable tissue remodeling and hence structure formation. Conversely, firm attachment to the substrate eventually leads to cell layers. Other models adopted a similar strategy in which a cell-populated 3D biopolymeric gel (mostly collagen or fibrin) is anchored between fixed posts. Basically, gel compaction caused by cell-generated contractile forces is constrained between the fixed posts, which produces a cylindrical gel under tension. Kapacee et al.[26] demonstrated that the establishment of tension in the fibrin gel between the posts is necessary for embryonic tendon cells to recapitulate in vitro the collagen deposition machinery that occurs in vivo during embryo development. Using an analogous model, Mienaltowski et al.[27] reported that tendon progenitor cells within contracting fibrin gels undergo morphological changes and assemble and organize collagen fibrils along the gel axis in which tension is generated. Additionally, collagen fibrils morphology and bundle compartmentalization follow patterns similar to those observed in the embryonic tissue.[28] Differently from external anchors, nanopatterning acts locally on FAs and cytoskelton assembly. This induces cells to form densely packed structures in which cells are elongated along the structure axis, which suggests that tension arising from cell contractility is uniaxial. Conversely, on flat substrates, cells organize in the form of spheroids in which the tension that builds up is isotropic causing a different structural evolution and cellular differentiation. Besides the direction of contractile forces, tension magnitude is also important for the tenogenesis process, because alteration of cell contractility with inhibitors affects the morphology of supracellular structures as well as the internal collagen organization. Tension establishing in compacting gels also proved to have major role into the differentiation of MSCs toward tenogenesis. Kuo and Tuan highlighted the role of Scleraxis in hMSCs tenogenesis in 3D collagen gel under tension.[29] In particular, Scleraxis was upregulated when cells were cultivated in the 3D gel and tension was sufficient to induce tenogenesis, but dynamic loading was necessary to sustain the tenogenic differentiation process of the hMSCs. Other tendon associated genes as Collagen 1 and 3 increased their expression level with culturing time even in static condition, which is in agreement with our data and support the hypothesis that cell generated contractile forces are necessary for both matrix gene expression and matrix assembly in the extracellular space. More recently, Kapacee et al.[30]

DOI: 10.1021/nl503737k
Nano Lett. XXXX, XXX, XXX−XXX

reported a different trend for the Scleraxis expression of hMSCs encapsulated in a fibrin gel under tension. No significant differences between 2D or 3D culture were observed in terms of Scleraxis expression. Therefore, other than dimensionality the proteinaceous environment in which the cells reside may exert a role in Scleraxis expression. In our experiments, even though tendon-like structures on the nanopattern or cell aggregates on flat surfaces are three-dimensional, they cannot be directly compared with conventional cell culture models in 3D exogenous matrices. However, even if we did not observe a significant upregulation of Scleraxis between the 1.4 μm pitch patterned and flat substrates, we believe that the levels of expression are sufficient to direct hMSCs toward a tenogenic differentiation pathway. In fact, Scleraxis is known to anticipate and regulate Tenomodulin expression.[31] Interestingly, we found that Scleraxis expression was increased after day 7 both on the 1.4 μm pitch pattern and flat substrates compared to undifferentiated hMSCs, by a factor 7 and 6, respectively (Supporting Information S11), while the late tendon markers tenomodulin and thrombospondin 4 remained almost undetectable (data not shown). Afterward, at day 10 the expression of Scleraxis declined and the negative trend held at day 15 when the expression was 1.8 and 1.6 fold on the nanopattern and flat surfaces, respectively, greater than undifferentiated cells. Even though we did not find any significant difference between expression levels of cells on the nanopattern and flat surfaces at each time point, the average values of Scleraxis expression were consistently higher for cells cultivated on the nanopattern. Conversely, tenomodulin and thrombospondin 4 were largely up-regulated in the presence of the 1.4 μm pitch pattern at 15 days. Finally, although both substrates support the differentiation of hMSCs toward mesodermal-derived fates, allowing the expression of early markers as Scleraxis, nevertheless only the nanopatterned substrate is able to drive the maturation of a predominant tenogenic phenotype, leading to the formation of tendon-like structures and to the up-regulation of late tendon markers (tenomodulin and thrombospondin 4). The observation that some of the nontendon-related markers were still expressed in the tendon-like structures demands that aspects of the chemical/physical properties of the nanopatterned material need to be finely tuned in order to further enhance hMSC tenogenic differentiation over other lineages.

Although we are aware that the underpinning biological mechanism is currently missing, we provided undeniable evidence of a material mediated tenogenesis, able to recapitulate in vitro crucial molecular and morphological events occurring during tendon development. In particular, by providing the initial conditions for FA assembly, hMSCs self-organize and produce tendon-like tissues in a deterministic manner. Our results open up new routes to the generation of functional tissues in vitro; in principle, by combining different arrays of patterns that control FA length and orientation and therefore cytoskeleton assembly, it would be possible to govern adhesive and contractile processes, thus guiding the spontaneous self-organization of stem cells and ultimately tissue-genesis.

■ ASSOCIATED CONTENT

Supporting Information

Materials and methods section, SEM examinations of the nanopatterned substrates used in the experimental campaign, brightfield images displaying hMSC behavior on both nanopatterned and flat substrates at different time-points, confocal images showing possible interactions between adjacent structures on nanopatterned or flat substrates, brightfield images displaying hMSC behavior on 0.7 μm pitch nanopatterned substrate, 1.4 μm pitch nanopatterned substrate treated with oxygen plasma, physisorbed fibronectin and covalently conjugated fibronectin, 1.4 μm pitch nanopatterned hard or soft substrate, 1.4 μm pitch nanopatterned polycarbonate substrate, brightfield images and confocal images of hMSCs treated with either ML-7 or Y-27632 contractility inhibitors, data on hMSC proliferation in the presence of the inhibitors, brightfield and polarized light microscopy images of Picrosirius Red stained structures under normal culturing conditions or in the presence of contractility inhibitors, additional TEM images of tendon-like structures formed on 1.4 μm pitch patterned substrates and of cell aggregates formed on flat substrates, multiphoton images of tendon-like structures formed in normal culturing condition or in the presence of contractility inhibitors, brightfield images of MC3T3, MG63, NIH 3T3, and HDF on 1.4 μm pitch patterned or flat substrates at different time points, kinetics of Scleraxis expression on 1.4 μm pitch patterned or flat substrates, videos and description of videos. This material is available free of charge via the Internet at http://pubs.acs.org.

■ AUTHOR INFORMATION

Corresponding Author

*E-mail: nettipa@unina.it.

Author Contributions

M.I., M.V., and P.A.N. designed, researched, and wrote the manuscript, M.I. and L.F. performed all the in vitro experiments and image acquisition, M.V. performed image analysis, and L.C. and E.J.P. carried out the RT-PCR experiments and analyzed and interpreted the data. All authors edited and approved the final manuscript.

Notes

The authors declare no competing financial interest.

■ ACKNOWLEDGMENTS

The authors thanks V. La Tilla and C. F. Natale for figure editing, D. Dannhauser for the helpful discussions, V. Mollo for processing samples for TEM, and R. Infranca for the advice on manuscript editing. This work was partly supported by FIRB project RBAP11BYNP "Newton".

■ REFERENCES

(1) Lancaster, M. A.; Renner, M.; Martin, C. A.; Wenzel, D.; Bicknell, L. S.; Hurles, M. E.; Homfray, T.; Penninger, J. M.; Jackson, A. P.; Knoblich, J. A. *Nature* **2013**, *501*, 373−390.

(2) Spence, J. R.; Mayhew, C. N.; Rankin, S. A.; Kuhar, M. F.; Vallance, J. E.; Tolle, K.; Hoskins, E. E.; Kalinichenko, V. V.; Wells, S. I.; Zorn, A. M.; Shroyer, N. F.; Wells, J. M. *Nature* **2011**, *470*, 105−109.

(3) Eiraku, M.; Takata, N.; Ishibashi, H.; Kawada, M.; Sakakura, E.; Okuda, S.; Sekiguchi, K.; Adachi, T.; Sasai, Y. *Nature* **2011**, *472*, 51−56.

(4) Lancaster, M. A.; Knoblich, J. A. *Science* **2014**, *345*, 1247125.

(5) Ader, M.; Tanaka, E. M. *Curr. Opin. Cell Biol.* **2014**, *31*, 23−28.

(6) Mammoto, T.; Ingber, D. E. *Development* **2010**, *137*, 1407−1420.

(7) Schwarz, U. S.; Gardel, M. L. *J. Cell. Sci.* **2012**, *125*, 3051−3060.

(8) Eyckmans, J.; Boudou, T.; Yu, X.; Chen, C. S. *Dev. Cell.* **2011**, *21*, 35−47.

DOI: 10.1021/nl503737k
Nano Lett. XXXX, XXX, XXX−XXX

(9) Teo, B. K. K.; Wong, S. T.; Lim, C. K.; Kung, T. Y. S.; Yap, C. H.; Ramagopal, Y.; Romer, L. H.; Yim, E. K. F. *ACS Nano* **2013**, *7*, 4785−4798.
(10) Engler, A. J.; Sen, S.; Sweeney, H. L.; Discher, D. E. *Cell* **2006**, *126*, 677−689.
(11) Natale, C. F.; Ventre, M.; Netti, P. A. *Biomaterials* **2014**, *35*, 2745−2751.
(12) Zeitouni, S.; Krause, U.; Clough, B. H.; Halderman, H.; Falster, A.; Blalock, D. T.; Chaput, C. D.; Sampson, H. W.; Gregory, C. A. *Sci. Transl. Med.* **2012**, *4*, 132−155.
(13) Narumiya, S.; Ishizaki, T.; Uehata, M. *Methods Enzymol.* **2000**, *325*, 273−284.
(14) Hale, C. M.; Sun, S. X.; Wirtz, D. *PLoS One* **2009**, *4*, e7054.
(15) Canty, E. G.; Starborg, T.; Lu, Y.; Humphries, S. M.; Holmes, D. F.; Meadows, R. S.; Huffman, A.; O'Toole, E. T.; Kadler, K. E. *J. Biol. Chem.* **2006**, *281*, 38592−38598.
(16) Kalson, N. S.; Starborg, T.; Lu, Y.; Mironov, A.; Humphries, S. M.; Holmes, D. F.; Kadler, K. E. *Proc. Natl. Acad. Sci. U.S.A.* **2013**, *110*, E4743−E4752.
(17) Schmitz, G.; Müller, G. *J. Lipid Res.* **1991**, *32*, 1539−1570.
(18) Kohama, M.; Nio, J.; Hashimoto, Y.; Iwanaga, T. *Jpn. J. Vet. Res.* **2002**, *50*, 125−139.
(19) Garfinkel, A.; Tintut, Y.; Petrasek, D.; Boström, K.; Demer, L. L. *Proc. Natl. Acad. Sci. U.S.A.* **2004**, *101*, 9247−9250.
(20) Chen, T. H.; Hsu, J. J.; Zhao, X.; Guo, C.; Wong, M. N.; Huang, Y.; Li, Z.; Garfinkel, A.; Ho, C. M.; Tintut, Y.; Demer, L. L. *Circ. Res.* **2012**, *110*, 551−559.
(21) Guillemette, M. D.; Cui, B.; Roy, E.; Gauvin, R.; Giasson, C. J.; Esch, M. B.; Carrier, P.; Deschambeault, A.; Dumoulin, M.; Toner, M.; Germain, L.; Veres, T.; Auger, F. A. *Integr. Biol.* **2009**, *1*, 196−204.
(22) Kim, D. H.; Lipke, E. A.; Kim, P.; Cheong, R.; Thompson, S.; Delannoy, M.; Suh, K. Y.; Tung, L.; Levchenko, A. *Proc. Natl. Acad. Sci. U.S.A.* **2010**, *107*, 565−570.
(23) Xing, Q.; Vogt, C.; Leong, K. W.; Zhao, F. *Adv. Funct. Mater.* **2014**, *24*, 3027−3035.
(24) Calve, S.; Dennis, R. G.; Kosnik, P. E.; Baar, K.; Grosh, K.; Arruda, E. M. *Tissue Eng.* **2004**, *10*, 755−761.
(25) Hairfield-Stein, M.; England, C.; Paek, H. J.; Gilbraith, K. B.; Dennis, R.; Boland, E.; Kosnik, P. *Tissue Eng.* **2007**, *13*, 703−710.
(26) Kapacee, Z.; Richardson, S. H.; Lu, Y.; Starborg, T.; Holmes, D. F.; Baar, K.; Kadler, K. E. *Matrix Biol.* **2008**, *27*, 371−375.
(27) Mienaltowski, M. J.; Adams, S. M.; Birk, D. E. *Tissue Eng., Part A* **2013**, *19*, 199−210.
(28) Mienaltowski, M. J.; Adams, S. M.; Birk, D. E. *Stem Cell Res. Ther.* **2014**, *5*, 86.
(29) Kuo, C. K.; Tuan, R. S. *Tissue Eng., Part A* **2008**, *14*, 1615−1627.
(30) Kapacee, Z.; Yeung, C. Y.; Lu, Y.; Crabtree, D.; Holmes, D. F.; Kadler, K. E. *Matrix Biol.* **2010**, *29*, 668−677.
(31) Shukunami, C.; Takimoto, A.; Oro, M.; Hiraki, Y. *Dev. Biol.* **2006**, *298*, 234−247.

DOI: 10.1021/nl503737k
Nano Lett. XXXX, XXX, XXX−XXX